SUPPLEMENTAL MATERIAL

Resonant stroboscopic Rydberg dressing: electron-motion coupling and multi-body interactions

Chris Nill[1,2], Sylvain de Léséleuc[3,4], Christian Groß[5], and Igor Lesanovsky[1,6]

[1]*Institut für Theoretische Physik and Center for Integrated Quantum Science and Technology, Universität Tübingen, Auf der Morgenstelle 14, 72076 Tübingen, Germany*
[2]*Institute for Applied Physics, University of Bonn, Wegelerstraße 8, 53115 Bonn, Germany*
[3]*Institute for Molecular Science, National Institutes of Natural Sciences, 444-8585 Okazaki, Japan*
[4]*RIKEN Center for Quantum Computing (RQC), 351-0198 Wako, Japan*
[5]*Physikalisches Institut and Center for Integrated Quantum Science and Technology, Universität Tübingen, Auf der Morgenstelle 14, 72076 Tübingen, Germany*
[6]*School of Physics and Astronomy and Centre for the Mathematics and Theoretical Physics of Quantum Non-Equilibrium Systems, The University of Nottingham, Nottingham, NG7 2RD, United Kingdom*

CONTENTS

I. ANALYSIS OF THE NON-ADIABATIC DRESSING PROTOCOL

A. Derivation of the time evolution operator $\mathcal{U}(T)$ at stroboscopic times

The non-adiabatic dressing sequence, see Fig. 1(b) in the main text, is decomposed into four phases. During the first one of duration τ_1, the system is described by the free evolution under the Rydberg Hamiltonian ($\hbar = 1$)

$$H_0 = \omega \sum_j a_j^\dagger a_j + V \sum_j n_j n_{j+1} + G \sum_j n_j n_{j+1}(x_j - x_{j+1}), \tag{S1}$$

where ω is the trapping frequency of the atoms with harmonic oscillator operators a_j and $a_j^\dagger$. The Rydberg interaction strength is parametrized by V, and the gradient of the potential by G. The projector onto an atom in Rydberg state $|r\rangle$ is given by $n_j = |r\rangle\langle r|_j$.

During the second phase of duration s, the laser Hamiltonian with Rabi frequency Ω and projected wave vector κ (the axis connecting the two atoms is the chosen as x-axis) is acing. This leads to the additional Hamiltonian

$$H_L = \sum_j \Omega \left(|\uparrow\rangle\langle r|_j \, e^{-i\kappa x_j} + |r\rangle\langle\uparrow|_j \, e^{i\kappa x_j} \right), \tag{S2}$$

where the position operator of atom j with atomic mass is

$$x_j = x_0(a_j + a_j^\dagger) = \sqrt{\frac{1}{2m\omega}}(a_j + a_j^\dagger). \tag{S3}$$

The Lamb-Dicke parameter is then given as $\eta = \kappa x_0$. During the third phase of the dressing sequence, with duration τ_2, only H_0 is acting (the laser is switched off), while during he fourth phase is the same as the second. Consequently, the time-evolution operator of a sequence of length $T = \tau_1 + \tau_2 + 2s$ is given by

$$\mathcal{U}_{\tau_1+\tau_2+2s} = \underbrace{e^{-is(H_L+H_0)}}_{\mathcal{U}_\pi} e^{-iH_0\tau_2} e^{-is(H_L+H_0)} e^{-iH_0\tau_1}. \tag{S4}$$

First, we evaluate now

$$\mathcal{U}_\pi = e^{-is(H_L+H_0)} \tag{S5}$$

$$= \exp\left\{ -is\Omega \sum_j \left(|\uparrow\rangle\langle r|_j \, e^{-i\kappa x_j} + |r\rangle\langle\uparrow|_j \, e^{i\kappa x_j} + \frac{\omega}{\Omega} a_j^\dagger a_j + \frac{V}{\Omega} n_j n_{j+1} + \frac{G_j}{\Omega} n_j n_{j+1}(x_j - x_{j+1}) \right) \right\}. \tag{S6}$$

We consider a strong laser driving which breaks the Rydberg blockade and is by magnitudes the largest energy scale with $V/\Omega \ll 1$, $\omega/\Omega \ll 1$, $G_j/\Omega \ll 1$, thus

$$\mathcal{U}_\pi = e^{-isH_L} = \exp\left\{ -is\Omega \sum_j \left(|\uparrow\rangle\langle r|_j \, e^{-i\kappa x_j} + |r\rangle\langle\uparrow|_j \, e^{i\kappa x_j} \right) \right\}. \tag{S7}$$

In addition, $\Omega s = \pi/2$ is chosen such that the laser performs π pulses, which reduce effectively to instantaneous pulses

$$\mathcal{U}_\pi = \prod_j \exp\left\{ -i\Omega s \left(|\uparrow\rangle\langle r|_j \, e^{-i\kappa x_j} + |r\rangle\langle\uparrow|_j \, e^{i\kappa x_j} \right) + 0 \cdot |\downarrow\rangle\langle\downarrow|_j \right\} \tag{S8}$$

$$= \prod_j \left[|\downarrow\rangle\langle\downarrow|_j - i \left(|\uparrow\rangle\langle r|_j \, e^{-i\kappa x_j} + |r\rangle\langle\uparrow|_j \, e^{i\kappa x_j} \right) \right]. \tag{S9}$$

The time-evolution operator from Eq. (S4) for a sequence reads then

$$\mathcal{U}_{\tau_1+\tau_2+2s} = \underbrace{\mathcal{U}_\pi e^{-iH_0\tau_2} \mathcal{U}_\pi}_{\mathcal{U}_\mathcal{R}} e^{-iH_0\tau_1}. \tag{S10}$$

The expression $\mathcal{U}_\mathcal{R}$ can be evaluated as

$$\mathcal{U}_\mathcal{R} = \mathcal{U}_\pi e^{-iH_0\tau_2} \mathcal{U}_\pi = \underbrace{\mathcal{U}_\pi \mathcal{U}_\pi}_{\prod_j (|\downarrow\rangle\langle\downarrow|_j - \mathcal{P}_j - n_j)} \mathcal{U}_\pi^\dagger e^{-iH_0\tau_2} \mathcal{U}_\pi \tag{S11}$$

$$= \prod_j \left(|\downarrow\rangle\langle\downarrow|_j - \mathcal{P}_j - n_j \right) \exp\left\{ -i\tau_2 \left(\omega \sum_j \underbrace{\mathcal{U}_\pi^\dagger a_j^\dagger a_j \mathcal{U}_\pi}_{A} + V \sum_j \underbrace{\mathcal{U}_\pi^\dagger n_j n_{j+1} \mathcal{U}_\pi}_{\mathcal{P}_j \mathcal{P}_{j+1}} + \sum_j G_j \underbrace{\mathcal{U}_\pi^\dagger n_j n_{j+1}(x_j - x_{j+1}) \mathcal{U}_\pi}_{\mathcal{P}_j \mathcal{P}_{j+1}(x_j - x_{j+1})} \right) \right\}, \tag{S12}$$

where we define the projector onto atom j in state $|\uparrow\rangle$ as $\mathcal{P}_j = |\uparrow\rangle\langle\uparrow|_j$. In addition,

$$A = \omega \left(a_j^\dagger a_j + i\eta(n_j - \mathcal{P}_j)(a_j - a_j^\dagger) + \eta^2(n_j + \mathcal{P}_j) \right). \tag{S13}$$

The time-evolution operator for a dressing sequence then is

$$\begin{aligned} \mathcal{U}_{\tau_1+\tau_2+2s} = & \left[\prod_j \left(|\downarrow\rangle\langle\downarrow|_j - \mathcal{P}_j - n_j \right) \right] \\ & \cdot \exp\left\{ -i\tau_2 \left(\omega \sum_j \left(a_j^\dagger a_j + i\eta(n_j - \mathcal{P}_j)(a_j - a_j^\dagger) + \eta^2(n_j + \mathcal{P}_j) \right) + \sum_j G_j \mathcal{P}_j \mathcal{P}_{j+1}(x_j - x_{j+1}) \right) \right\} \\ & \cdot \exp\left\{ -i\tau_1 \left(\omega \sum_j a_j^\dagger a_j + \sum_j G_j n_j n_{j+1}(x_j - x_{j+1}) \right) \right\} \\ & \cdot \exp\left\{ -i\tau_2 V \sum_j \mathcal{P}_j \mathcal{P}_{j+1} \right\} \cdot \exp\left\{ -i\tau_1 V \sum_j n_j n_{j+1} \right\}. \end{aligned} \tag{S14}$$

We consider an initial state $|\psi_0\rangle$ in which no Rydberg excitations are present. Thus, multiplying $\prod_j(\mathbb{1}-n_j)$ onto the time evolution does not affect the initial state. Since $\mathcal{U}_{\tau_1+\tau_2+2s}$ commutes with n_j, we can write

$$\mathcal{U}_{\tau_1+\tau_2+2s} = \mathcal{U}_{\tau_1+\tau_2+2s}\cdot\prod_j(\mathbb{1}-n_j) \tag{S15}$$

$$\begin{aligned}
&= \prod_j\left(|{\downarrow}\rangle\langle{\downarrow}|_j - \mathcal{P}_j\right)\exp\left\{-i\tau_2\left(\omega\sum_j\left(a_j^\dagger a_j - i\eta\mathcal{P}_j(a_j-a_j^\dagger)+\eta^2\mathcal{P}_j\right)+\sum_j G_j\mathcal{P}_j\mathcal{P}_{j+1}(x_j-x_{j+1})\right)\right\}\\
&\quad\cdot\exp\left\{-i\tau_1\omega\sum_j a_j^\dagger a_j\right\}\cdot\exp\left\{-i\tau_2 V\sum_j\mathcal{P}_j\mathcal{P}_{j+1}\right\}
\end{aligned} \tag{S16}$$

$$\begin{aligned}
&= \prod_j\left(|{\downarrow}\rangle\langle{\downarrow}|_j - \mathcal{P}_j\right)\\
&\quad\underbrace{\cdot\exp\left\{-i\tau_2\left(\omega\sum_j\left(a_j^\dagger a_j - i\eta\mathcal{P}_j(a_j-a_j^\dagger)+\eta^2\mathcal{P}_j\right)+\sum_j G_j\mathcal{P}_j\mathcal{P}_{j+1}(x_j-x_{j+1})\right)\right\}\cdot\exp\left\{i\tau_2\omega\sum_j a_j^\dagger a_j\right\}}_{\text{spin-motion coupling dynamics}}\\
&\quad\underbrace{\cdot\exp\left\{-i(\tau_1+\tau_2)\omega\sum_j a_j^\dagger a_j\right\}}_{\text{free-oscillator dynamics}}\underbrace{\cdot\exp\left\{-i(\tau_1+\tau_2)\frac{\tau_2 V}{\tau_1+\tau_2}\sum_j\mathcal{P}_j\mathcal{P}_{j+1}\right\}}_{\text{spin-spin dynamics}}.
\end{aligned} \tag{S17}$$

Gradient operator $\mathcal{G}_j$
Introducing the gradient operator enables us to commute the summands with

$$\begin{aligned}
\sum_j G_j\mathcal{P}_j\mathcal{P}_{j+1}(x_j-x_{j+1}) &= \sum_j G_j\mathcal{P}_j\mathcal{P}_{j+1}x_j - \sum_j G_j\mathcal{P}_j\mathcal{P}_{j+1}x_{j+1}\\
&= \sum_j G_j\mathcal{P}_j\mathcal{P}_{j+1}x_j - \sum_j G_{j-1}\mathcal{P}_{j-1}\mathcal{P}_j x_j\\
&= \sum_j\left(G_j\mathcal{P}_{j+1} - G_{j-1}\mathcal{P}_{j-1}\right)\mathcal{P}_j x_j\\
&= \sum_j\left(G_j\mathcal{P}_{j+1} - G_{j-1}\mathcal{P}_{j-1}\right)\mathcal{P}_j x_0(a_j+a_j^\dagger)\\
&=: \sum_j\mathcal{G}_j(a_j+a_j^\dagger).
\end{aligned} \tag{S18}$$

Note, that $[\mathcal{G}_j,\mathcal{G}_l]=0\,\forall j,l$ and $\mathcal{G}_j^2\neq\mathcal{G}_j$.

The spin-motion term (blue) can be further simplified using the gradient operator $\mathcal{G}_j$, see Eq. (S18), as

$$\exp\left\{-i\tau_2\left(\omega\sum_j\left(a_j^\dagger a_j - i\eta\mathcal{P}_j(a_j-a_j^\dagger)+\eta^2\mathcal{P}_j\right)+\sum_j G_j\mathcal{P}_j\mathcal{P}_{j+1}(x_j-x_{j+1})\right)\right\}\cdot\exp\left\{i\tau_2\omega\sum_j a_j^\dagger a_j\right\} \tag{S19}$$

and since all terms commute now in j

$$=\prod_j\exp\left\{-i\tau_2\left(\omega a_j^\dagger a_j - i\eta\omega\mathcal{P}_j(a_j-a_j^\dagger)+\eta^2\omega\mathcal{P}_j+\mathcal{G}_j(a_j+a_j^\dagger)\right)\right\}\cdot\exp\left\{i\tau_2\omega a_j^\dagger a_j\right\}. \tag{S20}$$

We complete the square with

$$= \prod_j \exp\left\{ -i\tau_2\omega \left[\left(a_j^\dagger \underbrace{-i\eta\mathcal{P}_j + \frac{\mathcal{G}_j}{\omega}}_{\mathcal{J}_j^\dagger} \right) \left(a_j + \underbrace{i\eta\mathcal{P}_j + \frac{\mathcal{G}_j}{\omega}}_{\mathcal{J}_j} \right) + \eta^2\mathcal{P}_j - \mathcal{J}_j^\dagger\mathcal{J}_j \right] \right\} \cdot \exp\left\{ i\tau_2\omega a_j^\dagger a_j \right\} \tag{S21}$$

$$= \prod_j \exp\Big\{ -i\tau_2\omega \left[(a_j + \mathcal{J}_j)^\dagger (a_j + \mathcal{J}_j) + \eta^2\mathcal{P}_j - \mathcal{J}_j^\dagger\mathcal{J}_j \right] \Big\} \cdot \exp\left\{ i\tau_2\omega a_j^\dagger a_j \right\} \tag{S22}$$

and introduce the displacement operator with $a + \alpha = \mathcal{D}^\dagger(\alpha) a \mathcal{D}(\alpha)$, thus

$$= \prod_j \exp\Big\{ -i\tau_2\omega \left[\left(\mathcal{D}^\dagger(\mathcal{J}_j) a_j \mathcal{D}(\mathcal{J}_j) \right)^\dagger \mathcal{D}^\dagger(\mathcal{J}_j) a_j \mathcal{D}(\mathcal{J}_j) + \eta^2\mathcal{P}_j - \mathcal{J}_j^\dagger\mathcal{J}_j \right] \Big\} \cdot \exp\left\{ i\tau_2\omega a_j^\dagger a_j \right\} \tag{S23}$$

$$= \prod_j \exp\left\{ -i\tau_2\omega \left[\mathcal{D}^\dagger(\mathcal{J}_j) a^\dagger \underbrace{\mathcal{D}(\mathcal{J}_j)\mathcal{D}^\dagger(\mathcal{J}_j)}_{\mathbb{1}} a \mathcal{D}(\mathcal{J}_j) + \eta^2\mathcal{P}_j - \mathcal{J}_j^\dagger\mathcal{J}_j \right] \right\} \cdot \exp\left\{ i\tau_2\omega a_j^\dagger a_j \right\}. \tag{S24}$$

Note that all terms in exp commute now, thus

$$= \prod_j \exp\Big\{ -i\tau_2\omega \left[\mathcal{D}^\dagger(\mathcal{J}_j) a_j^\dagger a_j \mathcal{D}(\mathcal{J}_j) \right] \Big\} \cdot \exp\left\{ i\tau_2\omega a_j^\dagger a_j \right\} \cdot \exp\left\{ -i\tau_2\omega \left(\eta^2\mathcal{P}_j - \mathcal{J}_j^\dagger\mathcal{J}_j \right) \right\}. \tag{S25}$$

Since $\mathcal{D}(\mathcal{J}_j)$ is a unitary operator and thus invertible it follows

$$= \prod_j \mathcal{D}^\dagger(\mathcal{J}_j) \underbrace{\mathrm{e}^{-i\tau_2\omega a_j^\dagger a_j} \mathcal{D}(\mathcal{J}_j) \mathrm{e}^{i\tau_2\omega a_j^\dagger a_j}}_{\text{Baker-Campbell-Hausdorff}} \cdot \exp\left\{ -i\tau_2\omega \left(\eta^2\mathcal{P}_j - \mathcal{J}_j^\dagger\mathcal{J}_j \right) \right\} \tag{S26}$$

$$= \prod_j \mathcal{D}^\dagger(\mathcal{J}_j) \exp\Big\{ \mathcal{J}_j e^{-i\tau_2\omega} a_j^\dagger - \mathcal{J}_j^\dagger e^{i\tau_2\omega} a_j) \Big\} \cdot \exp\left\{ -i\tau_2\omega \left(\eta^2\mathcal{P}_j - \mathcal{J}_j^\dagger\mathcal{J}_j \right) \right\} \tag{S27}$$

$$= \prod_j \mathcal{D}(-\mathcal{J}_j) \mathcal{D}\left(\mathcal{J}_j e^{-i\tau_2\omega} \right) \cdot \exp\left\{ -i\tau_2\omega \left(\eta^2\mathcal{P}_j - \mathcal{J}_j^\dagger\mathcal{J}_j \right) \right\} \tag{S28}$$

$$= \prod_j \exp\Big\{ -i\mathcal{J}_j^\dagger\mathcal{J}_j \sin(\omega\tau_2) - i\tau_2\omega \left(\eta^2\mathcal{P}_j - \mathcal{J}_j^\dagger\mathcal{J}_j \right) \Big\} \cdot \mathcal{D}\left(\mathcal{J}_j (e^{-i\omega\tau_2} - 1) \right) \tag{S29}$$

$$= \prod_j \exp\Big\{ -i\tau_2\omega \left[\mathcal{J}_j^\dagger\mathcal{J}_j \left(\mathrm{sinc}(\omega\tau_2) - 1 \right) + \eta^2\mathcal{P}_j \right] \Big\} \cdot \mathcal{D}\left(\mathcal{J}_j (e^{-i\omega\tau_2} - 1) \right) \tag{S30}$$

$$= \prod_j \exp\left\{ -i\tau_2\omega \left[\left(\frac{\mathcal{G}_j^2}{\omega^2} + \eta^2\mathcal{P}_j \right) \left(\mathrm{sinc}(\omega\tau_2) - 1 \right) + \eta^2\mathcal{P}_j \right] \right\} \cdot \mathcal{D}\left[\left(\frac{\mathcal{G}_j}{\omega} + i\eta\mathcal{P}_j \right) (e^{-i\omega\tau_2} - 1) \right]. \tag{S31}$$

If we insert this result now in Eq. (S17), we obtain

$$\mathcal{U}_{\tau_1+\tau_2+2s} = \prod_j (|\downarrow\rangle\langle\downarrow|_k - \mathcal{P}_j) \exp\left\{-i\tau_2\omega \left[\left(\frac{\mathcal{G}_j^2}{\omega^2} + \eta^2\mathcal{P}_j\right)(\mathrm{sinc}(\omega\tau_2) - 1) + \eta^2\mathcal{P}_j\right]\right\}$$
$$\cdot \exp\left\{-i(\tau_1+\tau_2)\frac{\tau_2 V}{\tau_1+\tau_2}\mathcal{P}_j\mathcal{P}_{j+1}\right\} \cdot \mathcal{D}\left[\left(\frac{\mathcal{G}_j}{\omega} + i\eta\mathcal{P}_j\right)(e^{-i\omega\tau_2} - 1)\right] \cdot \exp\left\{-i(\tau_1+\tau_2)\omega a_j^\dagger a_j\right\} \quad \text{(S32)}$$

$$= \prod_j (|\downarrow\rangle\langle\downarrow|_k - \mathcal{P}_j) \exp\left\{-i(\tau_1+\tau_2)\left[\frac{\tau_2 V}{\tau_1+\tau_2}\mathcal{P}_j\mathcal{P}_{j+1} + \frac{\mathcal{G}_j\tau_2}{\tau_1+\tau_2}\frac{\mathcal{G}_j}{\omega}(\mathrm{sinc}(\omega\tau_2) - 1) + \frac{\sin(\omega\tau_2)}{\tau_1+\tau_2}\eta^2\mathcal{P}_j\right]\right\}$$
$$\cdot \mathcal{D}\left[\left(\frac{\mathcal{G}_j}{\omega} + i\eta\mathcal{P}_j\right)(e^{-i\omega\tau_2} - 1)\right] \cdot \exp\left\{-i(\tau_1+\tau_2)\omega a_j^\dagger a_j\right\} \quad \text{(S33)}$$

$$= \prod_j e^{-i\pi\mathcal{P}_j} \exp\left\{-i(\tau_1+\tau_2)\left[\frac{\tau_2 V}{\tau_1+\tau_2}\mathcal{P}_j\mathcal{P}_{j+1} + \frac{\mathcal{G}_j\tau_2}{\tau_1+\tau_2}\frac{\mathcal{G}_j}{\omega}(\mathrm{sinc}(\omega\tau_2) - 1) + \frac{\sin(\omega\tau_2)}{\tau_1+\tau_2}\eta^2\mathcal{P}_j\right]\right\}$$
$$\cdot \mathcal{D}\left[\left(\frac{\mathcal{G}_j}{\omega} + i\eta\mathcal{P}_j\right)(e^{-i\omega\tau_2} - 1)\right] \cdot \exp\left\{-i(\tau_1+\tau_2)\omega a_j^\dagger a_j\right\} \quad \text{(S34)}$$

$$= \prod_j \exp\left\{-i(\tau_1+\tau_2)\left[\frac{\tau_2 V}{\tau_1+\tau_2}\mathcal{P}_j\mathcal{P}_{j+1} + \frac{\mathcal{G}_j\tau_2}{\tau_1+\tau_2}\frac{\mathcal{G}_j}{\omega}(\mathrm{sinc}(\omega\tau_2) - 1) + \frac{\sin(\omega\tau_2)}{\tau_1+\tau_2}\eta^2\mathcal{P}_j + \frac{\pi}{\tau_1+\tau_2}\mathcal{P}_j\right]\right\}$$
$$\cdot \mathcal{D}\left[\left(\frac{\mathcal{G}_j}{\omega} + i\eta\mathcal{P}_j\right)(e^{-i\omega\tau_2} - 1)\right] \cdot \exp\left\{-i(\tau_1+\tau_2)\omega a_j^\dagger a_j\right\}. \quad \text{(S35)}$$

We now again utilize the short laser pulses introduced earlier, see Eq. (S7). This allows us to write $T = \tau_1 + \tau_2 + 2s \approx \tau_1 + \tau_2$ to obtain the time evolution operator Eq. (5) of the main text,

$$\mathcal{U}(T) = \prod_j \underbrace{\exp\left\{-iT\left[\frac{\tau_2 V}{T}\mathcal{P}_j\mathcal{P}_{j+1} + \frac{\mathcal{G}_j\tau_2}{T}\frac{\mathcal{G}_j}{\omega}(\mathrm{sinc}(\omega\tau_2) - 1) + \frac{\sin(\omega\tau_2)\eta^2 + \pi}{T}\mathcal{P}_j\right]\right\}}_{\text{effective spin dynamics}}$$
$$\cdot \underbrace{\mathcal{D}\left[\left(\frac{\mathcal{G}_j}{\omega} + i\eta\mathcal{P}_j\right)(e^{-i\omega\tau_2} - 1)\right]}_{\text{spin-motion coupling}} \cdot \underbrace{\exp\left\{-iT\omega a_j^\dagger a_j\right\}}_{\text{free oscillator evolution}}. \quad \text{(S36)}$$

B. Spin decoherence due to spin-motion coupling under ultra-strong laser pulses

In this section, we investigate spin-motion coupling effects under ultra-strong laser pulses which are experimentally investigated in Ref. [1]. Here, the laser pulses are characterized by a large Rabi frequency $\Omega_0 \gg V$ that effectively overcomes the Rydberg interaction V. This interaction is much stronger than the trap frequency with $V \gg \omega$. As well as in the main text, each laser pulse is designed as a π pulse with $\Omega_0 s = \pi/2$, resulting in a tiny pulse duration s. Thus, for these ultra-strong pulses, the product $\omega\tau_2$ of the atomic oscillations becomes tiny, $\omega\tau_2 \ll 1$.

As shown in the main text, the system's time evolution operator $\mathcal{U}(T)$ simplifies (see Eq. (5) in the main text) when strictly $\omega\tau_2 = 0$, indicating that spin and oscillatory motion decouple. However, here we do not match this condition perfectly.

In order to understand the impact of residual spin-motion coupling in the limit $\omega\tau_2 \ll 1$, we perform the same study as in Fig. 2 of the main text. Specifically, we show the time evolution of S_x for small values of $\omega\tau_2$ in Fig. S1(a). We compare the exact evolution of S_x which includes spin-motion coupling (see Eq. (4) of main text) with the effective spin dynamics calculated by Eq. (6) of the main text. We observe that deviations during time evolution occur. In particular, the effective spin dynamics lead to periodic oscillations, while the exact dynamics show damped oscillations. This mismatch of exact- and effective spin dynamics, which here results in damped oscillations, can be interpreted as spin decoherence, which arises due to the entanglement between oscillatory degrees of freedom and spins. In Fig. S1(b), we reduce $\omega\tau_2$ by a factor of 200 compared to panel (a), while proportionally increasing V and G to maintain the effective interaction strength $V_{\text{eff}} = \tau_2 V/T$ and the effective gradient operator $\mathcal{G}_{j,\text{eff}} = \tau_2\mathcal{G}_j/T$. These effective quantities occur in the effective Hamiltonian, see Eq. (6) of the main text, and define the oscillation

envelopes of S_x. Compared to panel (a), we observe that the spin decoherence in S_x does not decrease and deviations between exact- and effective spin dynamics are still present in panel (b). This can be explained by expanding the collective displacement operator $\mathcal{J}_j$ (see main text). It couples spins and oscillatory motion and is the origin of the observed spin decoherence. For $\omega\tau_2 \ll 1$,

$$\mathcal{J}_j \approx -i\tau_2\mathcal{G}_j + \omega\tau_2\eta\mathcal{P}_j = -i\mathcal{G}_{j,\text{eff}} + \omega\tau_2\eta\mathcal{P}_j. \tag{S37}$$

As we show, $\mathcal{J}_j$ is dependent on the effective gradient operator $\mathcal{G}_{j,\text{eff}}$. Therefore, $\mathcal{J}_j$ remains unchanged for same $\mathcal{G}_{j,\text{eff}} = \tau_2\mathcal{G}_j$. This is why reducing $\omega\tau_2$ while increasing G does not reduce spin decoherence. On the other hand, reducing $\mathcal{G}_{j,\text{eff}}$ without changing $\omega\tau_2$ reduces spin decoherence. This means that by reducing the effective gradient, spin-motion coupling decreases, which ultimately removes spin decoherence as shown in Fig. S1(c).

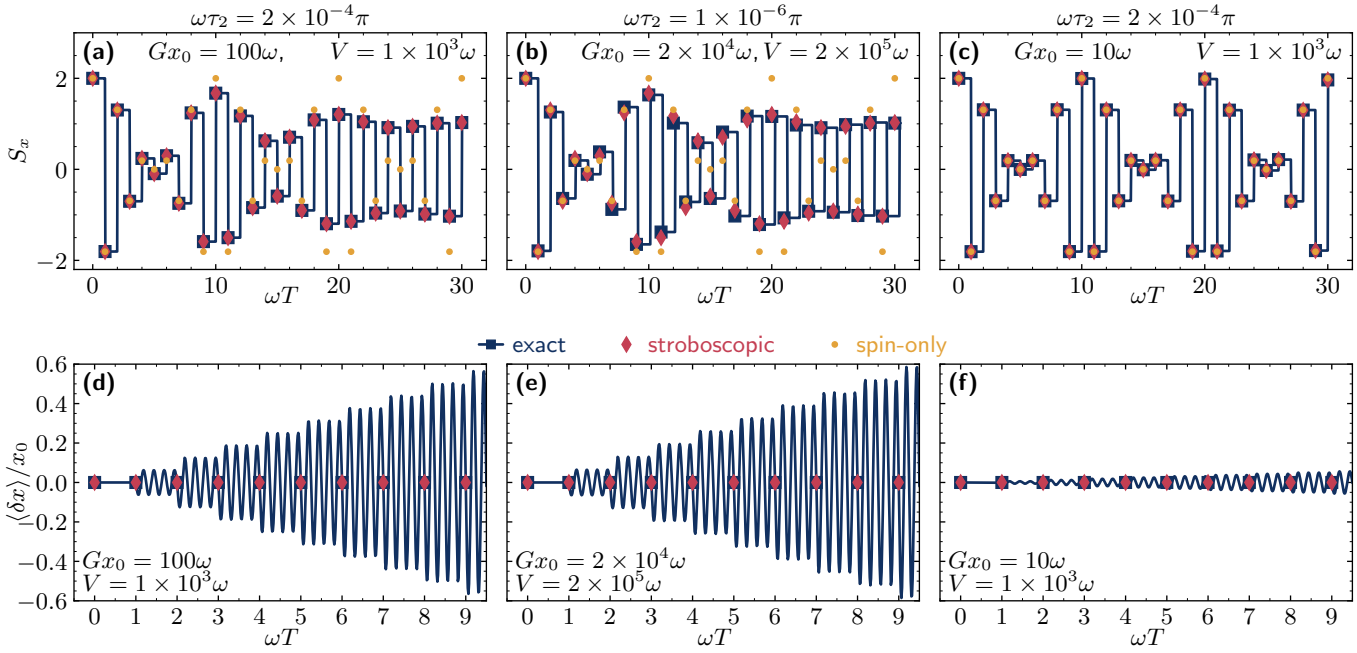

FIG. S1. **Spin-motion coupling for ultra-strong laser pulses. (a)** Exact- (blue) and effective spin dynamics (yellow) of S_x deviate significantly. Under the effective spin dynamics (Eq. (6) of the main text), periodic oscillations occur. However, due to spin-motion coupling, the exact dynamics (Eq. (4) of the main text) show damped oscillations which we associate with spin decoherence. Here, we set $\omega\tau_2 = 2\times10^{-4}$ and the Rydberg interaction $V = 1000\omega$. **(b)** Scaling down τ_2 and proportionally adjusting V and G cannot reduce spin decoherence in S_x compared to panel (a). **(c)** Reducing the effective gradient weakens spin decoherence, compared to (a) and (b). Thus, effective spin dynamics coincide with the exact dynamics. **(d)-(f)** The amplitude of the interatomic distance $\langle\delta x\rangle$ is mainly affected by the effective gradient $Gx_0\tau_2$ and impacts the observed spin decoherence. In all simulations the harmonic oscillator basis is truncated to contain a maximum of 5 excitations, the parameters values are $T = 8\pi/\omega$, $\eta = 0.6$ and $s = \pi/(2\times10^7\omega)$.

C. Decoupling spin-motion with a spin-motion echo

In the main text, we examined how adjusting the oscillation phase, $\omega\tau_2$, allows to decouple spin-motion dynamics. Here, we explore a complementary approach using a spin-motion echo. This method is based on setting the total sequence duration to satisfy $T = n\pi/\omega$ with n as an odd integer. The spin-motion echo relies on the application of two successive dressing sequences that enable the decoupling. Each sequence is describes by the time evolution operator $\mathcal{U}(T)$. To illustrate, we evaluate the time evolution operator, see Eq. (5) of the main text, for both successive

sequences

$$\begin{aligned}
\mathcal{U}^2(T=\frac{n\pi}{\omega}) &= \prod_j e^{-iTH_{j,\text{eff}}}\mathcal{D}(\mathcal{J}_j)e^{-iT\omega a_j^\dagger a_j}\cdot e^{-iTH_{j,\text{eff}}}\mathcal{D}(\mathcal{J}_j)e^{-iT\omega a_j^\dagger a_j} \\
&= \prod_j e^{-2iTH_{j,\text{eff}}}\mathcal{D}(\mathcal{J}_j)\underbrace{e^{-iT\omega a_j^\dagger a_j}\mathcal{D}(\mathcal{J}_j)e^{iT\omega a_j^\dagger a_j}}_{\text{Baker-Campbell-Hausdorff}}e^{-2iT\omega a_j^\dagger a_j} \\
&= \prod_j e^{-2iTH_{j,\text{eff}}}\mathcal{D}(\mathcal{J}_j)\mathcal{D}(\mathcal{J}_j e^{-i\pi n})e^{-2iT\omega a_j^\dagger a_j} \\
&= \prod_j e^{-2iTH_{j,\text{eff}}}\mathcal{D}(\underbrace{[1+e^{-i\pi n}]}_{=0,\text{ if } n \text{ is odd}}\mathcal{J}_j)e^{-2iT\omega a_j^\dagger a_j} \\
&= \prod_j e^{-2iTH_{j,\text{eff}}}e^{-2iT\omega a_j^\dagger a_j}.
\end{aligned} \tag{S38}$$

We see directly that spin-motion dynamics decouple under the chosen sequence duration for two successive applications of $\mathcal{U}(T)$. This justifies the spin-motion decoupling for the spin-motion echo.

II. ANALYSIS OF THE ADIABATIC DRESSING PROTOCOL

A. Adiabaticity and finite Rydberg lifetime: A case study

During the adiabatic dressing sequence, we require the state to be smoothly connected to the instantaneous eigenstates. This preserves the population of all basis states $\mathcal{C}$ after an adiabatic sequence. To quantify the adiabaticity of a sequence, we define the in-adiabaticity

$$\mathcal{E}(T) = 1 - \max_{\mathcal{C}} |\langle \mathcal{C}| \mathcal{U}(T) |\mathcal{C}\rangle|, \tag{S39}$$

where $\mathcal{C}$ is a basis state (configuration) of the Pauli z-basis. We evaluate $\mathcal{E}$ for all basis states and take the maximum. Importantly, $\mathcal{E}$ measures how adiabatic the dressing sequence is. For a completely adiabatic sequence, $\mathcal{E} = 0$. As we show later, increasing the sequence duration T improves the in-adiabaticity.

On the other hand, we excite Rydberg states coherently during the dressing sequence. With increasing sequence duration T, the spontaneous decay probability p increases as well, leading to higher decoherence. The decay probability p is approximately given by the time-integrated Rydberg excitation $\int_0^T \mathrm{d}t \sum_j \langle n_j \rangle (t)$ during the sequence with decay rate Γ of Rydberg state $|r\rangle$ as

$$p(\Omega_0 T) = 1 - \exp\left(-\Gamma \int_0^T \mathrm{d}t \sum_j \langle n_j \rangle (t)\right) \approx \Gamma \int_0^T \mathrm{d}t \sum_j \langle n_j \rangle (t). \tag{S40}$$

In order for the system to stay coherent during a dressing sequence, $p \ll 1$ is required. To demonstrate the trade-off between adiabaticity and decoherence due to sponatenoues decay, we study the system discussed in Fig. 3 of the main text in different parameter regimes, see Tab. I.

	Ω_0/Γ	Δ_0/Γ	Δ_1/Γ	V/Γ	ΓT	$\varphi_\uparrow/(2\pi)$	$\varphi_{\uparrow\uparrow}/(2\pi)$	$\varphi_{\uparrow\uparrow\uparrow}/(2\pi)$	p	$\mathcal{E}$
(**1**)	100	800	0	400	2.00	8.09	13.91	18.98	4.0×10^{-1}	7.9×10^{-08}
(**2**)	100	800	200	400	2.00	3.93	7.58	11.04	1.8×10^{-1}	1.6×10^{-07}
(**3**)	1000	8000	0	4000	0.20	8.09	13.91	18.98	4.0×10^{-2}	7.9×10^{-08}
(**4**)	1000	8000	0	8000	0.20	8.09	13.41	17.94	3.5×10^{-2}	2.3×10^{-07}
(**5**)	1000	8000	0	4000	0.05	4.05	6.96	9.49	9.9×10^{-3}	1.6×10^{-07}
(**6**)	1000	8000	0	4000	0.01	0.45	0.73	0.98	2.2×10^{-3}	4.3×10^{-02}

TABLE I. **Adiabaticity vs. decoherence from spontaneous decay of Rydberg states.** The rows (**1** − **6**) compare dressing sequences with different parameter sets with Rabi frequency Ω_0/Γ, detunings $\Delta_{0,1}$, interaction strength V and sequence duration ΓT scaled by the decay rate Γ. For all sets, we calculate the dynamical phases φ_α, see Eqs. (13) of the main text, the in-adiabaticity $\mathcal{E}$ and the decay probability p. (**1**) Resonant dressing sequence (Δ_1=0) for same parameters as in Fig. 3(b) of main text. Here, Rydberg states can be excited resonantly. (**2**) Compared to (1), for a dressing sequence which does not approach resonance ($\Delta_1 = 200\Gamma$), dynamical phases reduce. (**3**) In comparison to case (1), all parameters are scaled by increasing Ω_0. This decreases the decay probability p. (**4**) In comparison to case (3), increasing the interaction strength V, leads to decreased dynamical phases but improved $\mathcal{E}$. This can be explained by the changed energy spectrum of the system. (**5**) Compared to (3), a decreased sequence duration ΓT leads to lower p but worse $\mathcal{E}$, where the dynamic phases decrease. (**6**) A significantly longer sequence duration compared to (5), lowers p but increases the in-adiabaticity drastically.

B. Relative strength of multi-body interactions

The effective Hamiltonian of the adiabatic dressing sequence can be decomposed into contributions of k-body interactions. Their relative strengths are affected by the distance dependent Rydberg interaction $V(a_0)$. The three-body interaction strength $\mathcal{V}_3$ increases for shorter interatomic distance a_0. Increasing a_0, the two-body interaction strength starts dominating. This is seen in Fig. S2, where we show the ratio $\mathcal{V}_3/\mathcal{V}_2$.

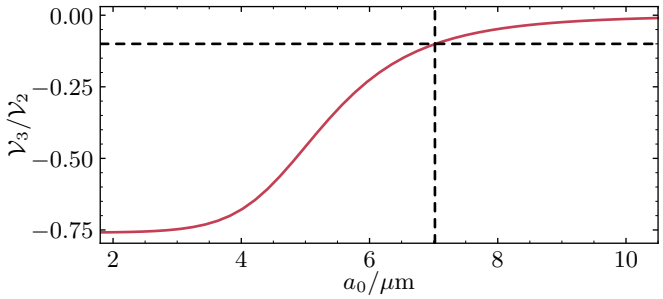

FIG. S2. **Ratio of three-body and two-body interaction strength.** Ratio of the three-body and two-body interaction strength $\mathcal{V}_3/\mathcal{V}_2$ for the parameters shown in Fig. 3(d) of the main text. With decreasing distance a_0, the three-body interaction dominates the two-body one. Specifically, for distances $a_0 \geq 7\,\mu$m, it is $\mathcal{V}_3 \leq 10/\mathcal{V}_2$.

C. Spin-motion coupling

In the main text, we consider an adiabatic dressing sequence of three spins without spin-motion coupling ($G = \eta = 0$). Now, we quantify the impact of finite spin-motion coupling and discuss under which conditions it becomes relevant. Therefore, we study a system of $N = 2$ spins coupled to a harmonic oscillator each. We analyze the spectrum of instantaneous eigenstates which illustrates the impact of the oscillatory energy levels. Additionally, we calculate the time evolution of the purity $P = \mathrm{tr}[(\mathrm{tr}_{\mathrm{osc}}[\rho(t)])^2]$ of the spin system, where $\mathrm{tr}_{\mathrm{osc}}$ is the partial trace over the oscillatory degrees of freedom and $\rho(t)$ the density matrix of the full quantum system. A purity of $P < 1$ signals entanglement between spin- and oscillatory degrees of freedom.

Figures S3(a-c) show the instantaneous eigenstates λ_α during a dressing sequence. Panel (a) shows the spectrum without spin-phonon coupling with the same parameters as in the main text. The introduction of harmonic oscillators subdivides the energy eigenstates into multiple with energy separation ω, see Figs. S3(b,c). A smaller separation of nearby eigenstates, leads to a higher transition probability between them during the sequence. This transitions ultimately lead to spin-motion entanglement. Thus, a longer sequence duration or an increased trapping frequency ω

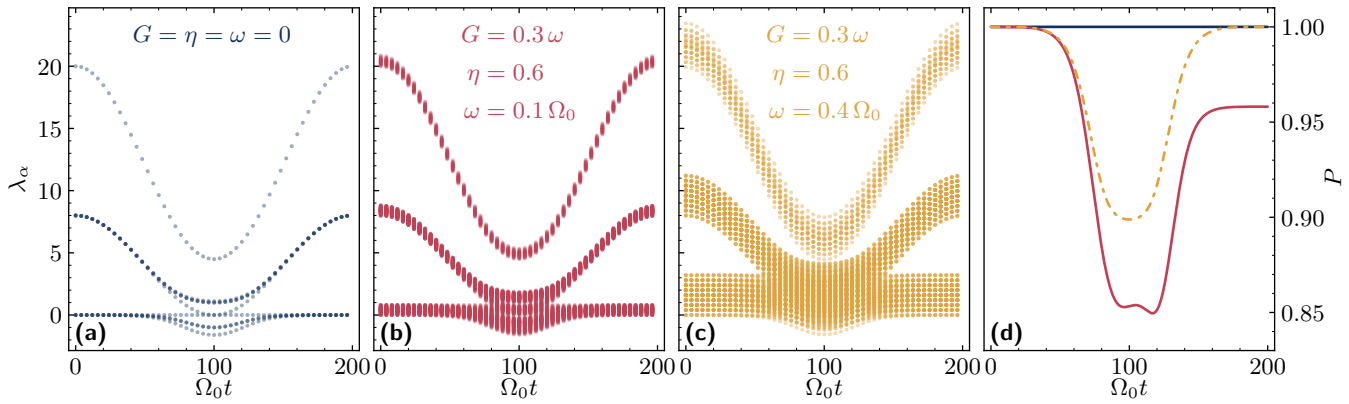

FIG. S3. **Impact of spin-motion coupling during a dressing sequence. (a)** Instantaneous eigenstates λ_α in the absence of spin-motion coupling for same parameters as in Fig. 3 of the main text. **(b)** The introduction of spin-motion coupling splits the eigenstates of different oscillator modes. The energy differences between neighboring levels is given by ω. **(c)** Increasing the trapping frequency ω increases the energy splitting and thus suppresses spin-motion entanglement. **(d)** Evolution of the spin purity P under these conditions: without spin-motion coupling (blue), P remains at one, indicating no spin-motion entanglement. Introducing spin-motion coupling with $\omega = 0.1\Omega_0$ leads to a purity of $P(T) = 0.958$ (red), meaning entanglement between spins and oscillators arises during the sequence. Increasing the trapping frequency ω, significantly reduces spin-motion coupling as confirmed by increased spin purity $P(T) \approx 1 - 3 \times 10^{-6}$. All simulations use $N = 2$ spins and a truncation of the harmonic oscillators up to 5 excitations each.

leads to less spin-motion entanglement.

In Fig. S3(d), we analyze the purity P of the three parameter sets. For no spin-motion coupling, the purity remains one during the whole sequence. Thus, the spins do not entangle with the motional degrees of freedom. For $\omega = 0.1\,\Omega_0$, we observe a decrease of the purity during the sequence until it finally reaches $P(T) = 0.958$ at the end of the sequence. Thus, spins and oscillators entangle during a dressing sequence. When increasing the trapping frequency to $\omega = 0.4\,\Omega_0$, the purity increases to $P(T) = 1 - 3 \times 10^{-6}$. Consequently, spin-motion entanglement can be reduced by increasing the trapping frequency.

[1] V. Bharti, S. Sugawa, M. Kunimi, V. S. Chauhan, T. P. Mahesh, M. Mizoguchi, T. Matsubara, T. Tomita, S. de Léséleuc, and K. Ohmori, Strong Spin-Motion Coupling in the Ultrafast Dynamics of Rydberg Atoms, Physical Review Letters **133**, 093405 (2024).